Fabrication of MnSO$_4$-doped PEPP Polymer and Investigation of its Structural and Electrical Properties

[1]Ravi H R, [2]Prasad N Bapat and [3*]Sajan C P

[1]Department of Physics, Post graduate and Research Centre, Bharathi College, Mandya-571422
[2]Department of Physics, PES Institute of Technology and Management, Shivamogga, Karnataka-577205
[3] VerdeEn Chemicals Pvt ltd, D-11, UPSIDC Industrial Area, Masoorie-Gulawati Road, Hapur District, Uttar Pradesh, India-201015

ABSTRACT: Polymers have been widely used as dielectric materials, passivation materials, capacitors, insulators, artificial muscle, and other applications in recent years. The in situ fabrication of commercial grade solid polymer polyethylene-polyprolyne complexes with manganese sulphate using the solution cast approach is reported in this article. Advanced characterisation tool such as microscopic study, XRD and FTIR measurements were used to investigate the structural properties of composite PEPP polymer films. FTIR spectra examinations for pure PEPP and complexes revealed the vibrational changes that occurred owing to the influence of dopant salt in the polymer, and XRD data demonstrated that the amorphous domains of the PEPP polymer matrix expanded in size as the MnSO$_4$ salt concentration rose. Under various frequency conditions, conductivity, dielectric constant, and AC conductivity were investigated. The conductivity investigation reveals that introducing Mn^{2+} ions into the polymer mix system improves the system's ionic conductivity. The AC conductivity under 1M frequency using PEPP polymer sample was 626.5 S/m, while using 1 percent MnSO$_4$doped PEPP sample the conductivity measured was 4807.7 S/m. We believe that these materials could be used in magnetic and/or optical devices, as well as the creation of solid state batteries and other electrochemical devices, based on the properties of the created material.

KEYWORDS:XRD, FTIR, polymer blend, Mn doping, electrical conductivity.

I. INTRODUCTION

A lot of research work has been done in the field of polymer or polymer blend additives in the past to produce and modify new materials of important value [1, 2]. Transition metal ion doped polymers are being investigated as promising materials for both theoretical and experimental research, and are becoming increasingly important as a result of their growing technological uses [3, 4]. The physical characteristics of polymer blends doped with transition metal ions are significantly altered. Physical properties of polymer blends are thought to be influenced by the chemical composition of dopants and the manner through which they interact with host matrices. [5, 6]. Because doped polymer mix films have potential features beneficial in advanced industrial applications, attention has been focused on their structural, thermal, and optical properties [7, 8].The presence of crystalline and amorphous zones, as well as the physical qualities that come from crystal amorphous interfacial effects, are essential features of PEPP [9]. Many research have been published in the literature on the electrical conductivity and dielectric properties of polymer blends in terms of the storage and dissipation of electric and magnetic energy in materials, which explains a variety of phenomena in optics, electronics, and solid state physics [10-12]. Dielectrics are used to store electric charges, while insulators are used to prevent electric charges from flowing [13, 14]. Dopants are added to polymer blends for a variety of purposes, including better processing, density control, optical effect, thermal conductivity, electrical and paramagnetic properties, and so on [15, 16].

Metal salts were utilized as dopants in the conductive polymer. These dopants have been identified to come into direct contact with polymer chains, inducing morphological changes in the polymer. The most common salts that elicit these

tendencies are NiCl2, EuCl3, and ZnCl2 [17]. Doping the polymer with various chemical agents and/or combining it with other standard low-weight plasticizers or polymer matrixes alter the polymer's characteristics [18]. Protonation of imine nitrogen atoms of the polymer backbone's quinoid group by protonic acids, Lewis acids, pseudo-protonation of the same sites by alkali metal ions, or oxidative doping at amine nitrogen atoms of benzenoid groups are examples of chemical agents that interact directly with the polymer chain [17]. Some compounds that aren't major dopants have been discovered to considerably increase the conductivity of a polymer, according to researchers. MnSO4 has been used as a dopant in polymer electrolyte sheets containing Poly (VinylAlcohol)[19, 20]. Similarly, Mn2+ ion doped polyaniline-metal nano composite and Mn2+ ion doped PVA/MAA:EA polymer blend films has also been reported [21, 22]. By forming electro active sites and changing their structural features, these chemicals have improved their electrical characteristics. We sought to develop MnSO4-doped PEPP polymer and investigate its structural and electrical properties in this paper.

II. MATERIALS AND METHODS

POLYPENCO Ltd. (UK) provided samples of polyethylene (PE) and polypropylene (PP) in the form of solid cylinders with a diameter of 2cm for PP and powder form for PE. The PP samples were cut into 1cm-long circular-shaped parallel solid blocks weighing 1 gram as received. Commercial $MnSO_4$ was utilised in this experiment. $MnSO_4$ was supplied by RANCHEM chemicals.

Fabrication ofMnSO₄-doped PEPP Polymer

Fabrication of $MnSO_4$-doped PEPP Polymer was done as illustrated in Fig 1. The solution cast method was used in the fabrication of MnSO4-doped PEPP polymer.The Stokes' law principle underpins the solution casting process. Polymer solution casting is a method of producing high-quality films with improved optical, mechanical, and physical properties. The polymer and prepolymer are mixed evenly and made soluble in the appropriate solution in this process. The matrix phase of the polymer dissolved readily in the solution, whereas the nanoparticles dispersed in the same or other solution. A known amount of weight $MnSO_4$ was dusted upon the 1 gram of PP and 1 gram of PE samples in a crucible. Throughout the experiment, 5ml of toluene, which functions as a solvent, was added to the crucible at 5-minute intervals. Toluene should be handled with caution. The crucible was heated in an oven at 150 ℃ for 70 minutes to ensure that $MnSO_4$ was completely dispersed throughout the polymer matrix. After cooling, the sample was cut into a different shaped parallel solid block, polished, and used. The samples were given names based on the amount of $MnSO_4$ applied by weight. PEPP refers to a sample that does not include $MnSO_4$. Samples containing $MnSO_4$ are classified as 0.20MnPEPP, 0.40MnPEPP, 0.60MnPEPP, 0.80MnPEPP, and 1.0 MnPEPP. In terms of a gram, the numbers represent the amount of $MnSO_4$ and PE PP applied. i.e. 0.20:1:1, where 1 represents PE and PP and 0.20 represents $MnSO_4$.
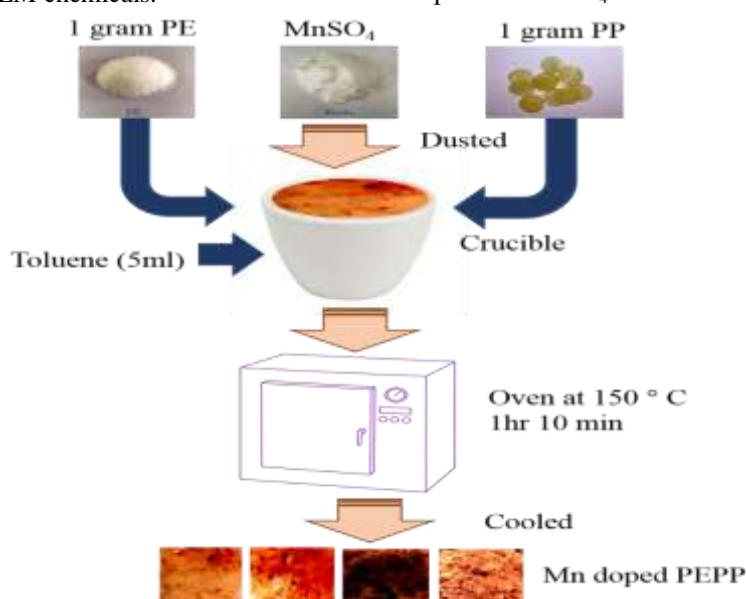
Figure 1. Schematic flowchart depicting the experimental procedure

III. INSTRUMENTS AND CHARACTERIZATION

A digital camera, a Sony cyber shot with a resolution of 8X, was used to study the physical appearance of the synthesised compound. To determine the dispersion of the substance within the polymer matrix, a laboratory microscope with a magnification of 100X was utilised. Powder X-ray diffraction investigations were performed on the RIGAKU Ultima III Series, TSX System, Japan XRD equipment. A Cu target generates Cu K radiation with a 40mA and 40kV operating current and voltage, respectively, in this equipment. The infrared spectra of the fabricated samples were recorded in the range of 4000 - 500 cm^{-1} using an FT-IR, JASCO 460 Plus spectrophotometer. At room temperature, the electrical conductivity of the ready samples was measured using the two probe method with a Keithly electrometer model 2400. With the use of an Impedance Analyzer (HP 4192A) with multi frequency at room temperature, the capacitance and Loss factor of the synthesised samples were measured using an LCR bridge interfaced in the frequency range 10K to 1M.

IV. RESULTS AND DISCUSSION
Morphological Studies

Morphological studies were carried out in order to comprehend the physical nature of the fabricated sample on doping (Fig 2). The detection of phase separation and interfaces using high resolution microscopic is frequently employed to investigate the compatibility of various components of polymer electrolytes[20]. Low resolution micrographic investigations were used to explore the physical changes that occur when MnSO$_4$ is introduced into the PEPP matrix (Fig 2a). When different weight percents of MnSO$_4$ are introduced, there are substantial differences in the physical appearance. As the weight percent of MnSO$_4$ increases, the transparent PEPP film changes from translucent to opaque. It was also discovered that as the MnSO$_4$ salt concentration increases, cross linking between the polymer increases, increasing the viscosity of the polymer, reducing its elasticity and making it rigid, which is consistent with Turkoz and Krul's findings. [23, 24]. The mechanical, thermal, and ionic conductivity of polymer electrolytes are heavily influenced by the compatibility of the polymer matrix and inorganic fillers. Microscopically, the morphology of pure PEPP and MnSO$_4$ doped PEPP polymer electrolytes is fairly homogeneous, but with varying degrees of roughness. The pure PEPP sample has no microscopic morphology that can be attributed to any crystalline form (shown in Fig.2). Semi-crystallisity nature was noticed when the MnSO4 concentration increased. The segregation of the dopant in the host matrix is shown by an increase in degree of roughness with increasing MnSO4 concentration. The phase segregation phenomenon in these complexed polymer electrolytes is clearly seen in our morphological analyses.

As a high resolution studies, the samples were examined under laboratory microscope at a magnification of 40X. It is evident from Fig.2b that the MnSO$_4$ that has been dusted upon the polymer film has not just been spread on the surface of the film but has been intruded and dispersed throughout the film. The addition of salts promotes crosslinking between the polymer and the salt, which affects the structural properties[24]. In the current study, the addition of varying amounts of MnSO$_4$ has an effect on the structural properties of the material in relation to the added amount of MnSO$_4$which is consistent with the findings of the XRD and FTIR studies.
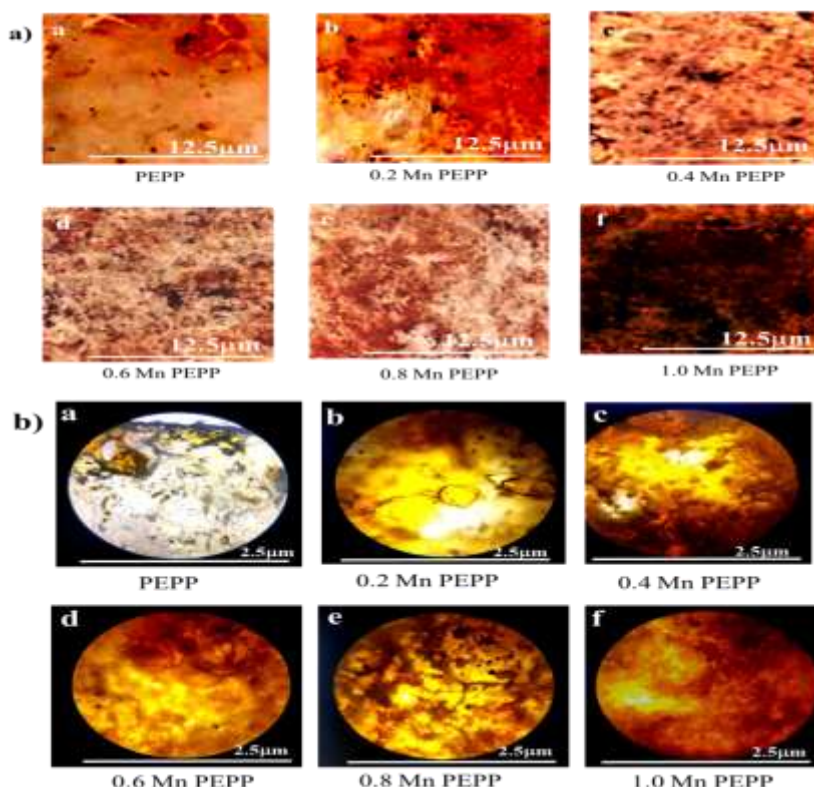
Figure 2. a) Low resolution micrographic studies of PEPP and MnPEPP samples and b) High resolution micrographic studies of PEPP and MnPEPP samples

XRD Studies

An X-ray diffraction was used to characterise the unprocessed materials. The XRD patterns of PE, PP, and $MnSO_4$ samples are shown in Figure 3a. The XRD pattern obtained was matched using PCPDFWIN software. The XRD patterns matches JCPDS file No 00-050-2397 for PP, 00-040-1995 for PE and 81-0018 for $MnSO_4$. The peaks at 14.33, 17.12, and 18.82 in the XRD pattern of PP correspond to the 110, 040, and 130 planes, respectively[25]. The planes 110, 200, 020, and 310 are represented by the numbers 21.56, 24.06, 36.44, and 41.00 in the PE XRD pattern [26]. $MnSO_4$ has an XRD pattern of 26.33, 27.74, 33.89, 43.44, which corresponds to planes 020, 112, 130, and 220 [27, 28]. All of the planes correspond to the PDF data.

The XRD pattern of PEPP and Mn-doped PEPP samples is shown in Fig. 3b. The Mn has been well intruded in the PEPP matrix, as seen in Fig 3b. We can see a few additional peaks in Fig 3 in addition to the PEPP peaks. These peaks are none other than $MnSO_4$ peaks. The $MnSO_4$ has been tightly bound within the PEPP polymer, as seen by the addition peaks. Meanwhile, we can see that the intensity of the $MnSO_4$ peaks has changed slightly. The amount of $MnSO_4$ introduced determines the intensity of the $MnSO_4$. The XRD patterns of PEPP, 0.40MnPEPP, and 0.60 MnPEPP are shown in Fig 3b. With the addition of $MnSO_4$, we can see a modest variation in peak intensity, indicating likely structural alterations within the polymer matrix. The pure PEPP has a characteristic peak, suggesting its semi-crystalline form, as can be seen in the graph. [29-31]. As the $MnSO_4$ content increases, the PEPP peaks become less strong. This could be caused by $MnSO_4$ disrupting the PEPP crystalline structure. Peaks about $MnSO_4$ salt occurred in the complexes, indicating that $MnSO_4$ salt dissolution in the polymer matrix was incomplete. When comparing pure PEPP films to $MnSO_4$ complexed PEPP films, the diffraction peaks are much more intense. Following the addition of $MnSO_4$, the degree of crystallinity of the polymer increased. Higher quantities of $MnSO_4$ salt in the polymer produced strong peaks, indicating that the crystalline phase was the dominant phase. This crystalline character leads to lower ionic diffusivity and ionic conductivity, which can be found in crystalline polymers with a stiff backbone [32].
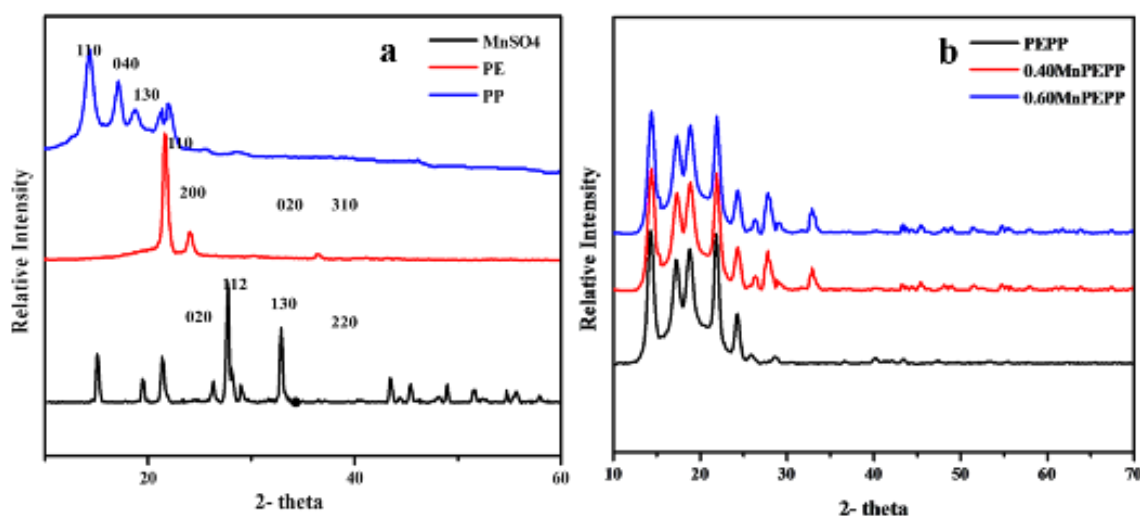
Figure 3. XRD pattern of a) PE, PP and MnSO4 samples and b) XRD pattern of PEPP and MnPEPP samples

FT-IR Spectroscopy Studies

Figure 4a shows the FT-IR spectra of pure PE, PP, and $MnSO_4$. The broadband of transmittance spectra at roughly 2,950, 2,920, and 2,840 cm^{-1} in the FT-IR spectra of PP is owing to the band's transmittance peak. Aromatic C–H stretching vibrations are represented by the bands at 2,950, 2,920, and 2,840 cm^{-1}[33]. The stretching of the C=O group is represented by the peak at 1716 cm^{-1}. A distinct peak is seen at around 3400 cm^{-1} due to the stretching of the O–H bond. There is a peak at 1255 cm^{-1} and two peaks around 950–990 cm^{-1} that can be attributed to C–O bond stretching and O–H out of plane vibration. The C=C bond is represented by the peaks around 1500–1650 cm^{-1}, and the =C–H group is represented by the peaks around 3100–3200 cm^{-1}. The aromatic C–H out of plane bending vibration of two adjacent hydrogen atoms was assigned the transmittance band at 841 cm^{-1} [34]. PE FT-IR spectra were mostly examined in the areas 3000–2800, 1550–1400, and 750–650 cm^{-1}. The typical absorbance bands for PE are 2914 cm^{-1}, 2847 cm^{-1}, 1470 cm^{-1}, and 718 cm^{-1}. PE is detected and quantified by measuring the 1470 cm^{-1} and 718 cm^{-1} peaks [35]. There are discrepancies in the absorption patterns of the samples between 1300 and 1400 cm^{-1}. There are three bands that can be assigned to the CH_2 and CH_3 groups: band I at 1377 cm^{-1}, band II at 1366 cm^{-1}, and band III at 1351 cm^{-1}. Peaks at 431, 418, and 408cm1 in the FT-IR spectra of $MnSO_4$ correspond to Mn IR absorbances. SO_4 corresponds to the band between 3700 and 3100 cm^{-1}[36].

The peaks in the range 2972-2860cm^{-1} in the pure PE-PP block copolymer sample (Fig. 4b) reveal that the >C-H stretching is present and that it is in the strong absorption zone, i.e. stretching mode of vibration. It can be found in the zone of significant absorption. In the middle absorption area, the peak at 1370cm^{-1} reflects CH_3 symmetric bending mode. The CH_3 asymmetric bending mode of vibration has a peak at 1462cm^{-1}, which is a medium absorption region, while vibration is evident at 980-960cm^{-1} for C-H out of plane bending, which is a low absorption region. At 2360cm^{-1}, there is a strong peak, which is a C-C stretching vibration. C-C stretching is shown by the peak at 2360cm^{-1}. In the middle absorption area, the peak at 1370cm^{-1} reflects CH_3 symmetric bending mode. The CH_3 asymmetric bending mode of vibration has a peak at 1462cm^{-1}, which is a medium absorption zone, and the C-H out of plane bending vibration has remained unchanged after doping at 980-960cm^{-1} [37-39]. The intermolecular hydrogen-bonded O-H stretching frequency of PEPP in MnPEPP samples is altered from 3250-2800 cm^{-1} to 3300-2850 cm^{-1}, 3320-2870 cm^{-1}. The changes in the IR spectrum with the addition of $MnSO_4$ has be shown in Fig 4b, confirming the efficient doping of $MnSO_4$ in changing the structural characteristic of the polymer, which is consistent with the XRD findings.
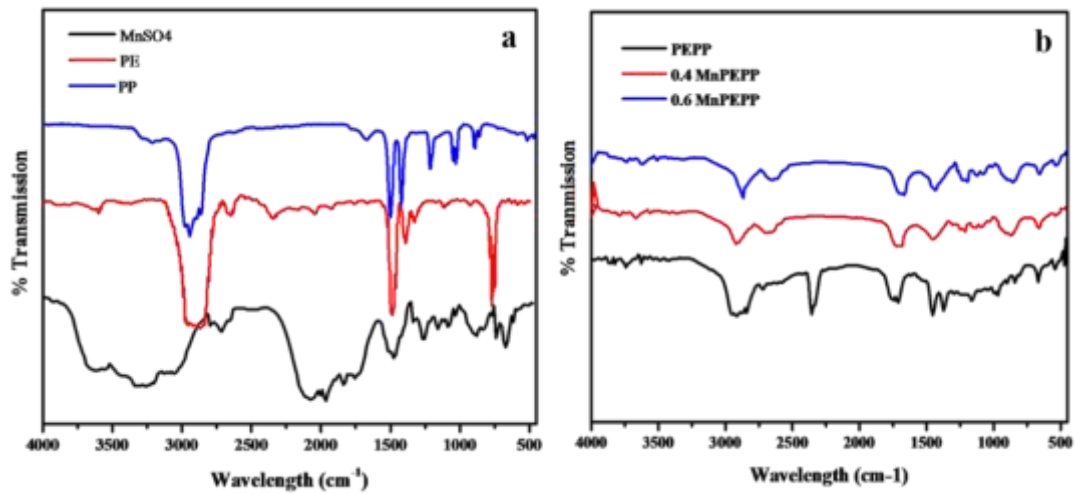
Figure 4. a) FT-IR spectra of PE, PP, and $MnSO_4$ and b) FT-IR spectra of PEPP and MnPEPP.

V. ELECTRICAL PROPERTIES STUDIES

DC conductivity

Table 1 summarizes the DC conductivity statistics. Conductivity vs. time graph MnPEPP concentration is indicated in Fig 5. In the instance of the PEPP sample, conductivity increases as Mn doping increases. The increase in ionic conductivity with increasing $MnSO_4$ concentration is attributed to a decrease in polymer film crystallinity as well as an increase in the number of mobile charge carriers [21, 40]. The addition of $MnSO_4$ reduces crystallinity within the PEPP matrix, which is responsible for the increase in ionic conductivity.

The more $MnSO_4$ is added, the more ions are formed, and hence the DC electrical conductivity rises. Increased electrical conductivity and lower activation energy values of polymer electrolytes can be explained by the fact that polymer films are known to be a mixture of amorphous and crystalline regions, with the amorphous region's features dominating the conductivity behaviour of such films[41]. Fast ion conducting pathways are provided by the connected network of amorphous areas, which increases ion mobility and thus ionic conductivity [42]. The greatest conductivity indicates the strongest and most efficient interaction between oxygen atoms and Mn^{2+} cations.
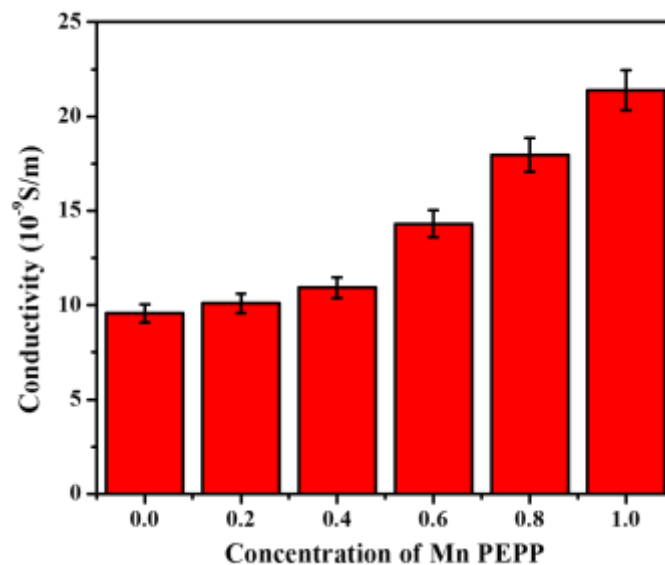
Figure 5. The DC Conductivity verses Concentration of PEPP and MnPEPP

Table 1. DC Conductivity v/s Concentration of MnPEPP

Sl. No.	Concentration of Mn PEPP	Conductivity (10^{-9}S/m)
1	0	9.56
2	0.2	10.10
3	0.4	10.93
4	0.6	14.30
5	0.8	17.97
6	1	21.38

Dielectric property

The dielectric characteristics were measured across a frequency range of 10 kHz to 1000 kHz. The results are given in table 2 correspondingly. Figure 6 shows the graphs of dielectric constant vs. frequency (10 kHz- 1000 kHz). The dielectric constant drops as the frequency increases, as shown in the graph. Meanwhile, we can see that the dielectric constant of MnPEPP samples is increasing with the added amount of $MnSO_4$. The dielectric constant increases as the concentration of $MnSO_4$ increases, implying that $MnSO_4$ plays a crucial role in improving the polymer's dielectric characteristic. As the dielectric constant rises, the density of states rises, and the band gap energy decreases, the conductivity of the system improves [5]. More charge carriers accumulate at internal interfaces when $MnSO_4$ concentrations rises, increasing interfacial polarisation and dielectric constant values. Charge traps and space-charge densities are also improved when $MnSO_4$ is loaded. It's worth noting that too much $MnSO_4$ in the polymer matrix might lead to a loss in conductivity by creating more charge recombination centers, which can lead to a decrease in interfacial polarisation.

The study of dielectric property describes how much charge a material can store, and it can be used to verify that an increase in conductivity is caused by an increase in charge carriers or free mobile ions. When a material's dielectric property improves, the amount of charge it can store improves as well [43]. The complex permittivity $\varepsilon^* = \varepsilon' - i\varepsilon''$ describes the dielectric response in general, with real ε' and imaginary ε'' components representing energy storage and loss in each cycle of applied electric field [16]. The availability of a high enough response time for dipole alignment could explain the minor rise in dielectric values at lower frequencies [44].
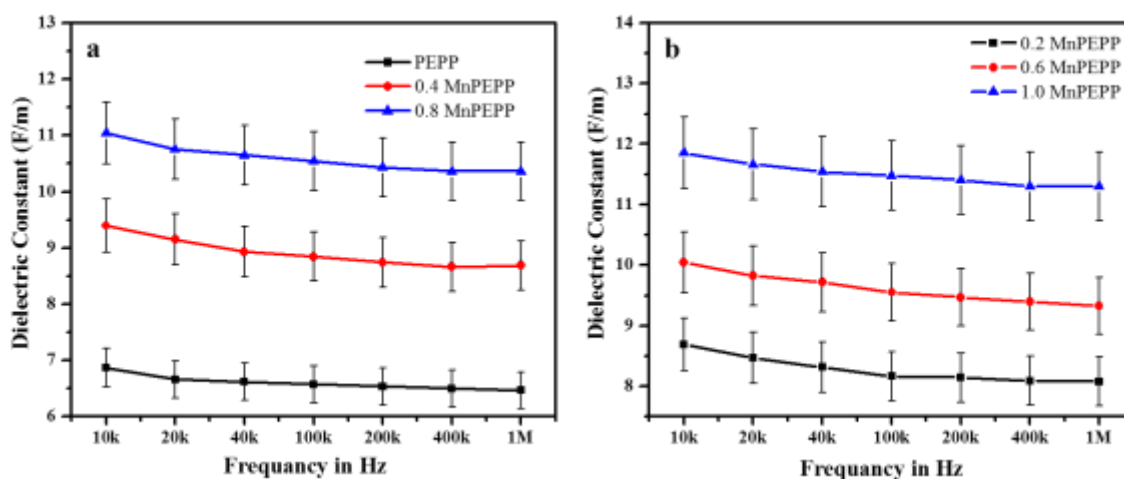
Figure 6. The Dielectric constant vs Frequency of PEPP and MnPEPP

Table 2. Dielectric constant (F/m)v/s Frequency

SL No	Frequency In Hz	0.0Mn PEPP	0.20Mn PEPP	0.40Mn PEPP	0.60Mn PEPP	0.80Mn PEPP	1.00Mn PEPP
1	10k	6.86	8.69	9.39	10.04	11.04	11.85
2	20k	6.66	8.46	9.14	9.82	10.75	11.66
3	40k	6.61	8.31	8.93	9.71	10.64	11.54
4	100k	6.57	8.16	8.84	9.55	10.54	11.48
5	200k	6.53	8.14	8.73	9.47	10.43	11.40
6	400k	6.49	8.09	8.66	9.39	10.36	11.30
7	1M	6.46	8.07	8.68	9.32	10.36	11.30

AC conductivity

Electrical conductivity is a useful experimental method for detecting structural flaws and crystalline solids' internal purity. Electrons, holes, and impurities are responsible for electrical conductivity, and so the mechanism of ionic conductivity may be explained [17]. At fault areas, some carriers are trapped, which explains why ionic materials have such low conductivity at room temperature[45]. A high-frequency alternating field must be used to promote conductivity[46]. Table 3 shows the σac values that were computed. Figure 7 depicts the fluctuation of σac with frequency (KHz). The graph shows that AC conductivity increases as frequency increases, but when MnSO$_4$ of various wt % was injected into the polymer matrix, conductivity increased with the added amount of MnSO$_4$. With the addition of MnSO$_4$, the conductivity increases, indicating that MnSO$_4$ plays an essential role in increasing the conductivity in polymers. The AC conductivity is a frequency dependent property, as seen in Fig 7, with the value rising marginally at low frequencies and exponentially rising at high frequencies, thus obeying the power law. Charge-induced deformations in the polymer, such as local vibrational modes or dielectric polarisation, lead to the creation of polarons as frequency increases. The moment of these polarons increases with frequency, resulting in greater conductivity. Inter and intra chain bouncing processes in the crystalline area enable the electrical conductivity of the synthesised product to vary. In the crystalline region, electrical conduction is caused by polaron bouncing, whereas in the amorphous zone, basic raw material resonant tunnelling is caused by tightly localised states [21].
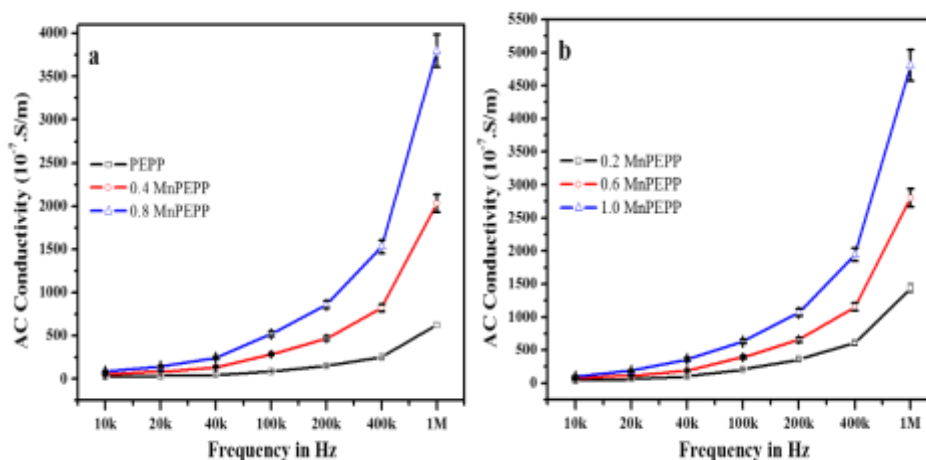
Figure 7. AC Conductivity of PEPP and MnPEPP samples

Table 3. AC conductivity v/s Frequency

Frequency (kHz)	AC Conductivity x10^{-7} (S/m)					
	0.0Mn PEPP	0.20Mn PEPP	0.40Mn PEPP	0.60Mn PEPP	0.80Mn PEPP	1.0Mn PEPP
10k	24.76	42.44	53.72	73.26	89.00	99.00
20k	34.24	62.60	85.87	113.05	147.14	187.14
40k	48.08	100.99	136.68	189.87	249.02	359.02
100k	90.68	207.46	286.18	394.43	522.62	632.62
200k	154.44	359.52	472.97	656.56	858.57	1068.57
400k	250.61	607.60	822.14	1154.12	1533.19	1943.19
1M	626.53	1436.25	2034.29	2802.43	3797.75	4807.75

CONCLUSION

According to the findings of the aforementioned study, the physical and chemical properties of PEPP change as the amount of $MnSO_4$ added rises. XRD and FT-IR measurements revealed that the addition of $MnSO_4$ affected the crystallinity and composition of PEPP. As the concentration of $MnSO_4$ increases, so does the DC electrical conductivity. Over a frequency range of 10kHz to 1000kHz, the dielectric constant increases as the amount of Mn increases. The AC-electrical conductivity increases with the addition of $MnSO_4$ over a frequency range of 10 kHz to 1000 kHz. The rise in conductivity with an increase in $MnSO_4$ concentration was attributed to an increase in amorphicity. These films exhibit a high sensitivity to doping/when a foreign material/salts like $MnSO_4$ is incorporated within them based on the results of these modifications, suggesting that they could be employed in magnetic and/or optical devices, as well as the fabrication of solid state batteries and other electrochemical devices. In the future, we intend to investigate the effect of other transition metals, such as Fe and Al, as doping materials on the thermal, structural, spectroscopic, and electrical properties of PEPP polymer blends.

CONFLICT OF INTEREST: Nil

REFERENCE
[1] Ojeda, T. "Polymers and the Environment". In: Yılmaz, F. (ed.) Polymer Science, p. 1-34. IntechOpen, Middle East Technical University, Turkey., 2013.

[2] Shen, J., Liang, J., Lin, X., Lin, H., Yu, J., Yang, Z., Chow, W.S. "Recent Progress in Polymer-Based Building Materials", Int. J. Polym. Sci., Vol. 2020, **p.** 1-15, 2020.

[3] K, N., Rout, C.S. "Conducting polymers: a comprehensive review on recent advances in synthesis, properties and applications", RSC Adv., Vol. 11, **p.** 5659-5697,2021.

[4] Le, T.H., Kim, Y., Yoon, H."Electrical and Electrochemical Properties of Conducting Polymers", Polymers., Vol. 9, **p.** 150-182, 2017.

[5] Aziz, S.B., Brza, M.A., Nofal, M.M., Abdulwahid, R.T., Hussen, S.A., Hussein, A.M., Karim, W.O. "A Comprehensive Review on Optical Properties of Polymer Electrolytes and Composites", Materials., Vol. 13, **p.** 3675-3729, 2020.

[6] Jancar, J., Douglas, J.F., Starr, F.W., Kumar, S.K., Cassagnau, P., Lesser, A.J., Sternstein, S.S., Buehler, M.J. "Current issues in research on structure–property relationships in polymer nanocomposites", Polymer., Vol. 51, **p.** 3321-3343, 2010.

[7] Beygisangchin, M., Abdul Rashid, S., Shafie, S., Sadrolhosseini, A.R., Lim, H.N. "Preparations, Properties, and Applications of Polyaniline and Polyaniline Thin Films-A Review", Polymers., Vol. 13, **p.** 2003-2049, 2021.

[8] Gueye, M.N., Carella, A., Faure-Vincent, J., Demadrille, R., Simonato, J.-P. "Progress in understanding structure and transport properties of PEDOT-based materials: A critical review", Prog. Mater. Sci., Vol. 108, **p.** 100616, 2020.

[9] Han, C.C., Shi, W., Jin, J. "Morphology and Crystallization of Crystalline/Amorphous Polymer Blends", In: Kar, K.K. (ed.) Polymers and Polymeric Composites: A Reference Series, p. 12000. Springer Berlin, Heidelberg., 2013.

[10] Pravakar, O., Siddaiah, T., Gopal, N.O., Ramu, C. "Structural, Optical and Electrical conductivity Studies of Mn2+ Ions Doped PVA/MAA: EA Polymer Blend Films", Int. J. Sci. res. Phy. App. Sci., Vol. 6, **p.** 80-87, 2018.

[11] Jia, Q., Huang, X., Wang, G., Diao, J., Jiang, P. "MoS2 Nanosheet Superstructures Based Polymer Composites for High-Dielectric and Electrical Energy Storage Applications". J. Phys. Chem. C., Vol. 120, **p.** 10206-10214, 2016.

[12] Jagadeesh Chandra, R.B., Shivamurthy, B., Kulkarni, S.D., Kumar, M.S. "Hybrid polymer composites for EMI shielding application- a review", Mater. Res. Express., Vol. 6, **p.** 082008-082068, 2019.

[13] Hongbo, L. "Dielectrics under Electric Field", In: Kandelousi, M.S. (ed.) Electric Field, pp. 322. IntechOpen, Babol Noshirvani University of Technology., 2018.

[14] Bar, V., Azaiza, E., Azaiza, D., Shirtz, A.S. "Emphasizing the Role of the Insulator in Electric Circuits: Toward a More Symmetric Approach to Insulator and Conductor in the Instruction of Electricity", World Journal of Educational Research., Vol. 3, **p.** 112-126 , 2016.

[15] Abdelaziz, M., Abdelrazek, E.M. "Effect of equal amounts of Mn and Co dopant addition on the structural, electrical and magnetic properties of PVDF films", Phys. B: Condens. Matter., Vol. 349, **p.** 84-91, 2004.

[16] Zapata-Arteaga, O., Perevedentsev, A., Marina, S., Martin, J., Reparaz, J.S., Campoy-Quiles, M. " Reduction of the Lattice Thermal Conductivity of Polymer Semiconductors by Molecular Doping", ACS Energy Lett., Vol. 5, **p.** 2972-2978, 2020.

[17] Dimitriev, O.P. "Doping of polyaniline by transition metal salts: effect of metal cation on the film morphology", Synth Met., Vol. 142, **p.** 299-303, 2004.

[18] Immergut, E.H., Mark, H.F.: Principles of Plasticization. In: Platzer, N.A.J. (ed.) Platzer; Plasticization and Plasticizer Processes, vol. 48, pp. 200. Advances in Chemistry; American Chemical Society, Washington, DC., 1965.

[19] Mohamed, R.I. "AC conductivity and dielectric constant of poly(vinyl alcohol) doped with MnSO4", J Phys Chem Solids., Vol. 61, **p.** 1357–1361, 2000.

[20] Reddy, S.M., Rao, S.S., Venkanna, N., Reddy, K.N. "Electrical and structural studies of pure and MnSO4 doped Poly (Vinyl Alcohol) polymer electrolyte films", Int. J. Chem. Anal. Sci., Vol. 2, **p.** 126-129, 2011.

[21] Pravakar, O., Siddaiah, T., Gopal, N.O., Ramu, C. "Structural, Optical and Electrical conductivity Studies of Mn2+ Ions Doped PVA/MAA: EA Polymer Blend Films", Int. J. Sci. res. Phy. app. Sci., Vol. 6, **p.** 80-87, 2018.

[22] Anju, C., Palatty, S. "Effect of Mn2+ as a redox additive on ternary doped polyaniline-metal nanocomposite: an efficient dielectric material", J. Mater. Sci.: Mater. Electron., Vol. 30, **p.** 21138-21149, 2019.

[23] Turkoz, E., Perazzo, A., Arnold, C.B., Stone, H.A. "Salt type and concentration affect the viscoelasticity of polyelectrolyte solutions", Applied Physics Letters., Vol. 112, p.203701-203704, 2018.

[24] Krul, L.P., Nareiko, E.I., Matusevich, Y.I., Yakimtsova, L.B., Matusevich, V., Seeber, W. "Water super absorbents based on copolymers of acrylamide with sodium acrylate", Polymer Bulletin., Vol. 45, **p.**159–165, 2000.

[25] Benabid, F.Z., Kharchi, N., Zouai, F., Mourad, A.-H.I., Benachour, D. "Impact of co-mixing technique and surface modification of ZnO nanoparticles using stearic acid on their dispersion into HDPE to produce HDPE/ZnO nanocomposites", Polym. Polym. Compos., Vol. 27, **p.** 389-399, 2019.

[26] Wang, S., Ajji, A., Guo, S., Xiong, C. "Preparation of Microporous Polypropylene/Titanium Dioxide Composite Membranes with Enhanced Electrolyte Uptake Capability via Melt Extruding and Stretching", Polymers.,Vol. 9, **p.** 101-112, 2017.

[27] Zhao, Z., Liu, J., Xia, W., Cao, C., Chen, X., Huo, G., Chen, A., Li, H. "Removal of molybdenum from MnSO4 solution with freshly precipitated "nascent" Mn3O4", Hydrometallurgy.,Vol. 99, **p.** 67-71, 2009.

[28] Chen, H., Wang, K., Ming, X., Zhan, F., Muhammad, Y., Wei, Y., Li, W., Zhan, H. "The Efficient Removal of Calcium and Magnesium Ions from Industrial Manganese Sulfate Solution through the Integrated Application of Concentrated Sulfuric Acid and Ethanol", Metals.,Vol. 11, **p.** 1339-1349, 2021.

[29] Krumova, M., Lo´pez, D., Benavente, R., Mijangos, C., Peren˜a, J.M. "Effect of crosslinking on the mechanical and thermal properties of poly(vinyl alcohol)", Polymer.,Vol. 41, p. 9265–9272, 2000.

[30] Huang, S.-J., Lee, H.-K., Kang, W.-H. "Proton Conducting Behavior of a Novel Composite Based on Phosphosilicate/Poly(Vinyl Alcohol)", J. Korean Ceram. Soc., Vol. 42, **p.** 77-80, 2005.

[31] Madhava Kumar, Y., Bhagyasree, K., Gopal, N.O., Ramu, C., Nagabhushana, H. "Structural, Thermal and Optical Properties of Mn2+ Doped Methacrylic Acid – Ethyl Acrylate (MAA:EA) Copolymer Films", Z Phys Chem (N F)., Vol. 231, **p.** 1039-1055, 2017.

[32] Mohamad, A.A., Mohamed, N.S., Yahya, M.Z.A., Othman, R., Ramesh, S., Alias, Y., Arofa, A.K. " Ionic conductivity studies of poly(vinyl alcohol) alkaline solid polymer electrolyte and its use in nickel–zinc cells", Solid State Ion., Vol. 156, **p.** 171–177, 2003.

[33] Wieczorek, W., Stevens, J.R., Florjahczyk, Z. "Composite polyether based solid electrolytes. The Lewis acid-base approach", Solid State Ion., Vol. 85, **p.** 67-72, 1996.

[34] Gopanna, A., Mandapati, R.N., Thomas, S.P., Rajan, K., Chavali, M. "Fourier transform infrared spectroscopy (FTIR), Raman spectroscopy and wide-angle X-ray scattering (WAXS) of polypropylene (PP)/cyclic olefin copolymer (COC) blends for qualitative and quantitative analysis", Polym., Vol. 76, p. 4259-4274, 2018.

[35] Gulmine, J.V., Janissek, P.R., Heise, H.M., Akcelrud, L. "Polyethylene characterization by FTIR", Polym Test., Vol. 21, **p.** 557–563, 2002.

[36] Anupriya, K.G., Hemalatha, P. "Effect of ZnSO4 and MnSO4 on the Growth of Sulphamic Acid Single Crystals", Mat. Sci. Res. India., Vol. 15, **p.** 151-158, 2018.

[37] P.Sagunthala, P.Yasotha, L.Vijaya. "Growth and Characterization of Manganese (II) Sulphate and L-Lysine doped Manganese (II) Sulphate (LMnSO4) Crystals", Int. J. Sci. Eng. App., Vol. 1, **p.** 46-52, 2013.

[38] Cunha, C.B.d., Lopes, P.P., Mayer, F.D., Hoffmann, R. "Assessment of Chemical and Mechanical Properties of Polymers Aiming to Replace the Stainless Steel in Distillation Column", Mater., Vol. 21, **p.** e20170679-e20170689, 2018.

[39] Sarker, M., Rashid, M.M., Molla, M. "Abundant High-Density Polyethylene (HDPE-2) Turns into Fuel by Using of HZSM-5 Catalyst", Journal of Fundamentals of Renewable Energy and Applications., Vol. 1, **p.** 1-12, 2011.

[40] Sreekanth, K., Siddaiah, T., Gopal, N.O., Jyothi, N.K., Kumar, K.V., Ramu, C. "Thermal, Structural, Optical and Electrical Conductivity studies of pure and Mn2+ doped PVP films". S. Afr. J.Chem. Eng., Vol. 36, **p.** 8-16, 2021.

[41] Khare, P.K., Jain, S.K., Paliwal, S.K. "Conduction mechanism in doped polymethyl methacrylate (PMMA) films", Bull. Mater. Sci., Vol. 20, **p.** 699-705, 1997.

[42] Aziz, S.B., Woo, T.J., Kadir, M.F.Z., Ahmed, H.M. "A conceptual review on polymer electrolytes and ion transport models",. J Sci-Adv Mater Dev., Vol. 3, **p.** 1-17, 2018.

[43] Hao, X. " A review on the dielectric materials for high energy-storage application", J. Adv. Dielectr., Vol. 3, **p.** 1330001-1330014, 2013.

[44] Stillinger, F.H. "Low Frequency Dielectric Properties of Liquid and Solid Water", In: Lebowitz, E.W.M.a.J.L. (ed.) The liquid state of matter: Fluids, Simple and Complex, pp. 341-431. North-Holland Publishing Company, Murray Hill, New Jersey U.S.A., 1982.

[45] B, S., HG, B., P, S., J, O. "Electrical Properties". In: Czichos, H., Saito, T., Smith, L. (eds.) Springer Handbook of Materials Measurement Methods, pp. XXVI, 1208. Springer, Berlin, Heidelberg., 2006

[46] Bouaamlat, H., Hadi, N., Belghiti, N., Sadki, H., Naciri Bennani, M., Abdi, F., Lamcharfi, T.-d., Bouachrine, M., Abarkan, M. "Dielectric Properties, AC Conductivity, and Electric Modulus Analysis of Bulk Ethylcarbazole-Terphenyl", Adv. Mater. Sci. Eng., Vol. 2020, **p.** 1-8, 2020.